

## ELECTROCHEMICAL AND SPECTRAL STUDY OF THE HEMIN-SURFACTANT INTERACTION IN SOLUTION

Ana Maria TOADER and Elena VOLANSCHI\*

Department of Physical Chemistry, University of Bucharest, Blvd Elisabeta 4-12, Bucharest RO-030018, Roumania  
E-mail: volae@gw-chimie.math.unibuc.ro

Received February 19, 2007

The hemin - SDS interaction was studied by cyclic and linear voltammetry with stationary and rotating disc electrode, as well as by absorption spectroscopy. The spectral results outline three processes, in function of the surfactant concentration. Processes I and III were assigned to the interaction between hemin and the molecular SDS, and respectively, between hemin and the SDS micelle and were characterized quantitatively by a 1:1 stoichiometry and the binding constants. The transition region between these processes corresponds to the aggregation domain of the surfactant in presence of hemin, preponderantly dimeric in solution. In electrochemical experiments, due to the higher concentration of hemin and electrolyte favoring the autoaggregation of hemin, only process III is observed and characterised by the binding constant and the diffusion coefficients of the free and bound hemin.

### INTRODUCTION

Hemin ( $\text{Fe}^{\text{III}}$  Protoporphyrin IX), oxidized state of heme (Fig. 1), is known to be a very active component in biological media, having many functions in free state, associated with specific proteins or nucleic acids.<sup>1, 2</sup> Hemin is the active cofactor for a variety of enzymes implied in different biological redox processes, such as catalases, peroxidases and monooxygenases.<sup>3</sup>

It should be noted that natural porphyrins are sparingly soluble in water at low pH and undergo extensive aggregation at alkaline pH. One of the

simple but useful techniques to avoid the aggregation and dimer formation of heme is the utilization of detergents. It is known that, in the presence of sodium dodecyl sulphate, (SDS) in aqueous medium, hemin is encapsulated as monomer in surfactant micelles.<sup>4</sup> Previous literature studies have shown that electrochemical studies on aqueous surfactant solutions are less complicated by chemical reactions preceding or succeeding the electron transfer step. It was shown that hemin in micelles is more stable to aggregation or hydrolysis leading to dimers connected by oxo bridges.<sup>5</sup>

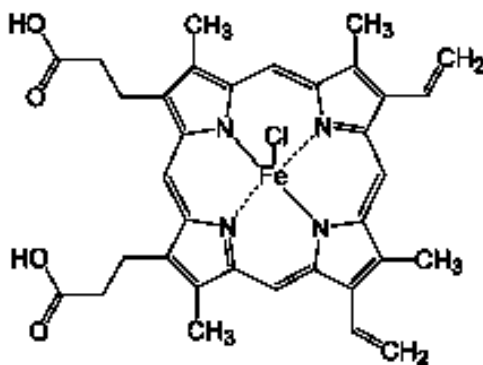


Fig. 1 – The chemical structure of hemin.

The use of aqueous surfactant solutions in electrochemical studies on heme model compounds is justified because it mimics the hydrophobic microenvironment around heme in an essentially aqueous medium. Monomer heme can therefore be studied by electrochemical techniques in aqueous solutions under conditions similar to those in heme proteins.

The object of the present paper concerns the study of the hemin – SDS interaction, by cyclic voltammetry and UV-VIS spectral experiments, in aqueous solutions in presence of 0.1 M KNO<sub>3</sub> and to elucidate the nature of this interaction. The association constant and the diffusion coefficients of free and bound hemin characterize the hemin – SDS binding equilibrium.

Coupled electrochemical (cyclic voltammetry with stationary and rotating glassy carbon disc electrode - RDE) and UV-VIS spectral methods were employed. As the spectral methods are more specific and sensitive to the structure modifications, their use in conjunction with electrochemical methods allows getting a deeper insight in the mechanism of this interaction.

## RESULTS AND DISCUSSION

### A. Electrochemical results

#### 1. Hemin in aqueous solution

Electrochemistry of hems in aqueous solutions is complicated by solubility restrictions and aggregation behaviour. Previous literature data have shown that the behaviour of hemin in aqueous media is strongly dependent on the experimental conditions. It was supposed that hemin undergoes a reversible reduction and the overall reaction is a two-electron process, iron (III) dimer to iron (II) monomer, with the reduction product of the dimer in alkaline solution being strongly adsorbed at the electrode.<sup>6</sup> When the ionic strength of the medium was 0.1 M and the concentration of hemin *ca.* 1 mM, a diffusion-controlled process was also detected in the pH range 7-13.<sup>7</sup>

Cyclic and RDE linear voltammetric curves of hemin in aqueous solutions in presence of 0.1 M KNO<sub>3</sub> are presented in Fig. 2a, b. The results show that the electrochemical reduction of hemin in aqueous solution supposes two monoelectronic transfer steps around -0.615 V *vs.* SCE (at 0.05 Vs<sup>-1</sup>) and -1.1 V *vs.* SCE assigned to the reduction at the

central ion Fe<sup>III</sup> to Fe<sup>II</sup> respectively Fe<sup>II</sup> to Fe<sup>I</sup>.<sup>8-10</sup> Analysis of the RDE curves in Fig. 2b verifies the monoelectronicity of the first wave.

The slope of the plot log *i*<sub>pc</sub> *vs.* log *v* is a good criterion to distinguish between adsorption and diffusion waves. For the first reduction wave of hemin recorded in our work conditions, the slope of 1.36 in aqueous solutions (for the second wave 0.94) is indication for an adsorption on glassy carbon electrode in aqueous media (inset fig. 2a).

Adsorption peaks can occur along with diffusion peaks, the extent of overlap being determined by the relative strength of adsorption of the oxidized and reduced species.<sup>11</sup>

In order to verify this assignment, the peak current in cyclic voltammetry at low scan rate (0.02 Vs<sup>-1</sup>) was represented in function of time and the typical adsorption isotherm was obtained (data not shown). Moreover, if the electrode hold for about three hours in the hemin solution (3.45x10<sup>-3</sup> M) is introduced in a 0.1 M KNO<sub>3</sub> solution without hemin, the cyclic voltammograms in Fig 3 are obtained. Analysis of the anodic and cathodic peak currents shows a behaviour characteristic for a weakly adsorbed reduction product: the formal potential is located at positive values *vs.* the diffusion wave, the slope of the plot log *i*<sub>pa</sub> *vs.* log *v* is 0.95 (*r*<sup>2</sup> = 0.997, *n* = 7), the ratio *i*<sub>pa</sub>/*i*<sub>pc</sub> is greater than unity and increases (from 0.94 to 2.35) with increasing scan rate (inset fig. 3).<sup>12</sup>

The superficial concentration of the adsorbed electroactive species,  $\Gamma$ , is given by the equation:<sup>13</sup>

$$i_p = \frac{n^2 F^2 A \Gamma}{4RT} \cdot v \quad (1)$$

where: *i*<sub>p</sub> is the cathodic peak current, *n* is the number of electrons, *A* the electrode area, and *v* the scan rate in Vs<sup>-1</sup>. A value of  $\Gamma = 2.23 \times 10^{-9}$  molcm<sup>-2</sup> was obtained for the superficial concentration of the adsorbed hemin from the slope of the linear dependence of the peak current *vs.* scan rate according to eq. (1).

Alternative determination of the adsorbed species concentration may be performed by the integration of the cathodic current at low scan rate. Using this method, a value of 4.3x10<sup>-10</sup> mol/cm<sup>2</sup> at scan rate 0.02 Vs<sup>-1</sup> was obtained.<sup>14</sup> The great difference between the results could be an indication that the adsorption prewave is superimposed on a diffusion wave, and both processes are contributing to the measured current.

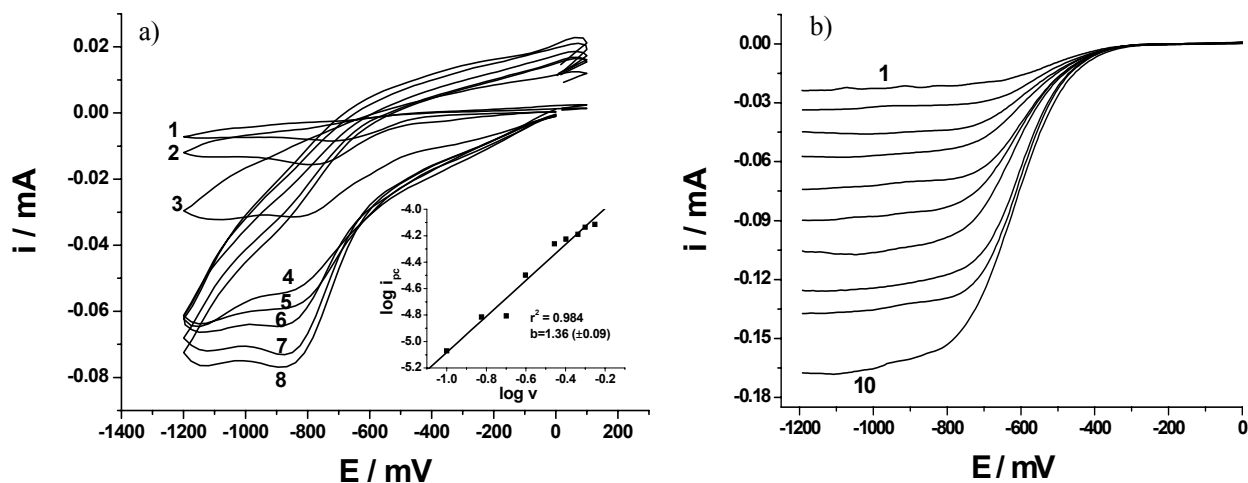


Fig. 2 – Hemin ( $c = 3.54 \text{ mM}$ ) in aqueous solution with  $0.1 \text{ KNO}_3$  supporting electrolyte: a) cyclic voltammograms in the range of potential scan rate  $0.1 - 0.56 \text{ V/s}$ ; (inset – logarithmic dependence of the peak current,  $\log i_{pc}$ , on the potential scan rate,  $\log v$ ); b) RDE at  $\omega = 100 - 4500 \text{ rpm}$  (1-10).

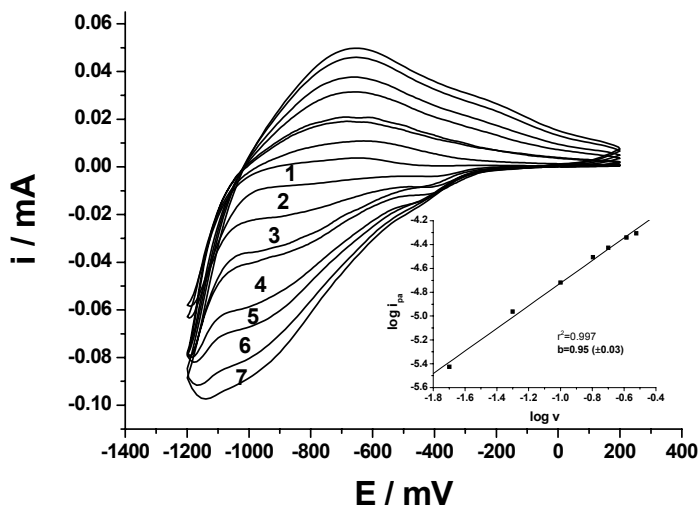


Fig. 3 – Cyclic voltammograms recorded with the electrode introduced in a  $0.1 \text{ M KNO}_3$  solution without hemin, after it was held for about three hours in the hemin solution ( $3.45 \times 10^{-3} \text{ M}$ ), in the range of potential scan rate  $0.02 - 0.3 \text{ V/s}$ ; inset - logarithmic dependence of the peak current  $\log i_{pa}$  on the potential scan rate,  $\log v$ .

As the system studied belongs to that category where reduction product is adsorbed, and electrode reaction is irreversible, we may use Laviron's equation:<sup>15</sup>

$$E_p = E^0 + \frac{RT}{\alpha nF} \ln \frac{RTk_s}{\alpha nF} - \frac{RT}{\alpha nF} \ln v \quad (2)$$

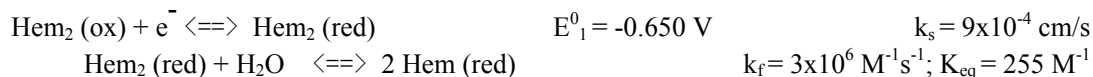
where:  $\alpha$  is the electron transfer coefficient,  $k_s$  the standard rate constant of the surface reaction,  $v$  the scan rate and  $E^0$  the formal potential. According to eq. (2), the plot of  $E_p$  vs.  $\ln v$  should be linear. From its slope (Fig. 4), the  $\alpha n$  value can be determined, and from the intercept, the  $k_s$  can be calculated, if the value of  $E^0$  is known. The value of  $E^0$  can be

determined from the plot of  $E_p$  vs.  $v$ , by extrapolating the line to  $v = 0$  ( $E^0 = -0.538 \text{ V}$ ). Values of  $\alpha n = 0.2$  and  $k_s = 0.24 \text{ s}^{-1}$  were obtained.

## 2. Hemin – SDS interaction

Fig. 5 shows the recorded voltammograms of the hemin solution, in the absence (a) and presence of different SDS concentrations.

Analysis of the first reduction wave in the absence of surfactant (curve a), using the DigiSim simulation gives a good agreement with the experimental results in the range  $0 \div -0.9 \text{ V}$  (Fig. 5 – inset up) supposing an EC mechanism:



where A stands for the hemin-dimer, B, for the reduced hemin-dimer, and C for the reduced hemin-monomer. The starting parameter values,  $\alpha = 0.3$  and diffusion coefficient  $D = 4.5 \cdot 10^{-7} \text{ cm}^2 \text{ s}^{-1}$ ,

are justified by the preliminary analysis of the experimental data ( $\alpha = 0.24$ , from  $|E_p - E_{p/2}| = 47.7/\alpha \text{ mV}^{12}$ ) and by the value of the diffusion coefficient from literature data in similar conditions.<sup>5,9</sup>

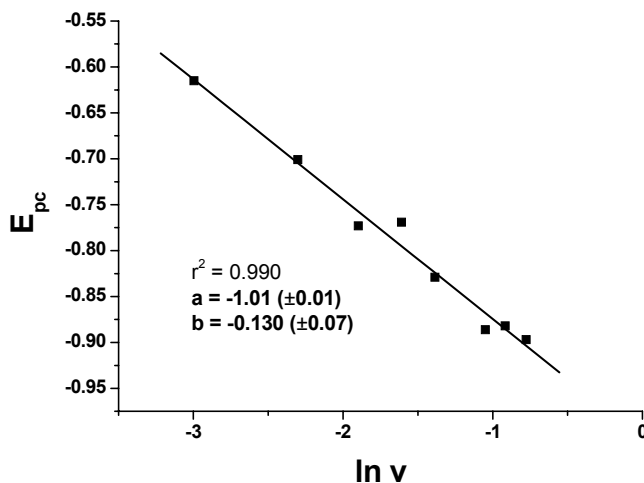


Fig. 4 – Semilogarithmic dependence of the peak potential  $E_{pc}$  on the potential scan rate  $\ln v$  for 3.54 mM hemin; other conditions were the same as in Fig. 2.

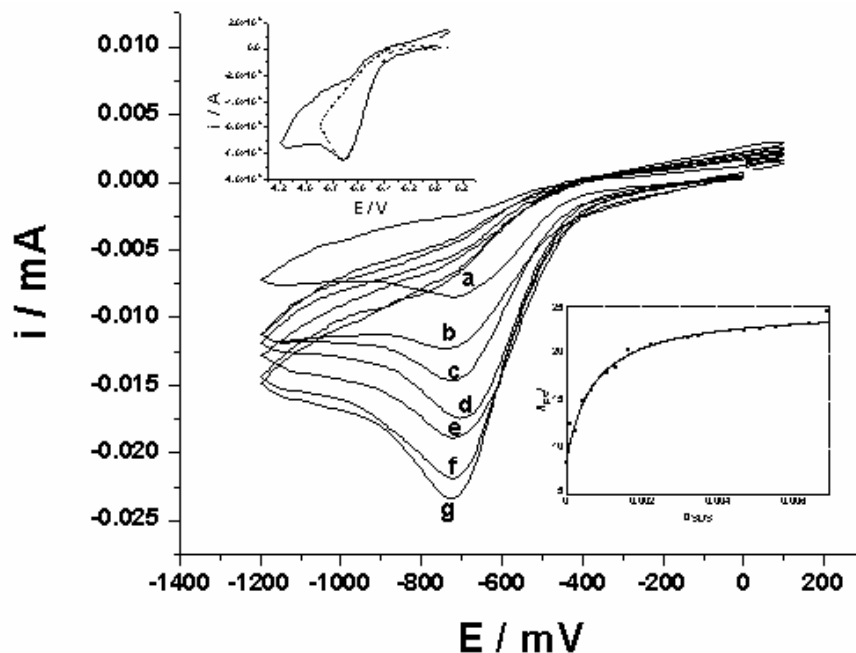


Fig. 5 – Cyclic voltammograms of hemin in absence and in the presence of SDS at different concentration: (a) 0 mM; (b) 0.1 mM; (c) 0.4 mM; (d) 1 mM; (e) 2 mM; (f) 5 mM; (g) 7 mM; incubation time: 4 min.; potential range  $-1.2 \text{ V} \div 0.2 \text{ V}$ ; potential scan rate 100 mV/s; *inset – up*: DigiSim simulation of the first reduction wave with the parameters in the text (dash dot-simulated, line-experimental); *inset – down*: Binding curve of hemin to SDS; points represent experimental peak current,  $|i_{pc}|$  and the solid curve represents the best fit with eq. [7].

The results attest to a slow electron transfer ( $k_s = 9 \times 10^{-4} \text{ cm s}^{-1}$ ), followed by a pseudo first order rapid chemical reaction, most probably the dissociation of the reduced dimer of hemin to the monomer, in agreement with literature data previously discussed.<sup>6</sup>

Comparison of the  $E^0$  value obtained by simulation (-0.650 V) with the formal potential of the adsorption wave (-0.538 V) shows that the adsorption wave appears at a more positive potential, meaning that the reduction product is adsorbed. The difference between these values is low enough (0.112 V) to allow overlapping of the two processes and rendering the analysis more difficult.

As the SDS concentration increases, up to 2 mM, caused the peak potential of the first wave,  $E_p$ , to shift to more positive potentials (c, d curves in fig. 5); whereas, going to higher SDS concentrations (e – g curves) had the opposite effect, similar with literature data on hemoglobin.<sup>16</sup> The shift to more positive potential values means that the reduced form of hemin is stabilized by the interaction with SDS. Simultaneously the cathodic peak current increases up to a saturation value.

The increase of the cathodic current could be the result of the existence of a multilayer of weakly adsorbed hemin on the electrode surface. Also, it could be due to the formation of the hemin - SDS electroactive complex.

If the final product of reduction is iron (II) monomer hemin, as shown by literature data<sup>6</sup> and DigiSim simulation, then the hemin monomer in reduced form interacts with the SDS micelle.

Using cyclic voltammetry in the study of molecular interactions, information may be obtained from current values ( $i_p, i_i$ ).

The interaction of hemin with the SDS micelle may be described as follows:



The binding constant,  $K$ , for the above equilibrium is given by:

$$K = \frac{c_{\text{H-SDS}}}{c_{\text{H}} \times c_{\text{SDS}}} = \frac{c_b}{(c_{\text{H}}^0 - c_b) \times c_{\text{T}}^{\text{SDS}}} \quad (4)$$

where:  $c_b$  is the bound hemin concentration,  $c_{\text{H}}^0$  is the initial hemin concentration and  $c_{\text{T}}^{\text{SDS}}$  is the SDS total concentration.

The peak current expression for an irreversible wave is given by:

$$I = 2.99 \times 10^5 \times \alpha^{1/2} n^{1/2} A D_0^{1/2} c_{\text{H}}^0 \nu^{1/2} \quad (5)$$

where:  $n$  is the number of electrons,  $A$  the electrode area,  $\nu$  the sweep rate,  $D_0$  the diffusion

coefficient of the electroactive species and  $\alpha$  is the electron transfer coefficient. The increase of the current during complexation (encapsulation) may be due to the formation of the hemin - SDS electroactive species, and to the increase of the solubility of hemin in presence of surfactant.

Considering that the total hemin concentration is  $c_{\text{H}}^0 = c_b + c_f$ , we can write

$$I_{\text{T}} = B \times [D_f^{1/2} c_f + D_b^{1/2} c_b] = B \times [D_f^{1/2} c_{\text{H}}^0 - (D_f^{1/2} - D_b^{1/2}) c_b] \quad (6)$$

where:  $B$  represents all the constants, and  $D_f$  and  $D_b$  are the diffusion coefficients of the free and bound hemin, respectively. Replacing the  $c_b$  concentration determined from the equilibrium eq. (4), the current  $I_0$  in the absence of SDS ( $I_0 = B \times D_f^{1/2} \times c_{\text{H}}^0$ ) and the current  $I_{\text{complex}}$  corresponding to a solution containing SDS in excess ( $I_{\text{complex}} = B \times D_b^{1/2} \times c_b$ ) the current expression becomes:

$$i = \frac{i_0 + i_{\text{complex}} \times K \times c_{\text{T}}^{\text{SDS}}}{1 + K \times c_{\text{T}}^{\text{SDS}}} \quad (7)$$

The dependence of the cathodic peak current on the SDS concentration is presented in Figure 5 – inset down. A nonlinear regression fit of the experimental data with equation (7) yielded the following results:

$K = (1.39 \pm 0.14) \times 10^3 \text{ M}^{-1}$ . Using  $I_{\text{complex}}$  obtained by nonlinear fitting, a value of  $D_b = 6.72 \times 10^{-6} \text{ cm}^2 \text{ s}^{-1}$  is obtained.

Analysis of the hemin-SDS complex by cyclic voltammetry shows that the reduction process is controlled by diffusion (a value of 0.29 is obtained for the slope of the plot  $\log i_{\text{pc}}$  vs.  $\log \nu$  (not shown)). The diffusion coefficient of the hemin-SDS complex calculated from the slope of the plot  $i$  vs.  $\nu^{1/2}$  (eq. (5)) is  $D_b = 0.17 \times 10^{-6} \text{ cm}^2 \text{ s}^{-1}$ . Both these values are about an order of magnitude higher than the diffusion coefficient reported for hemin in aqueous solutions in the pH range 8-10, where the hemin dimers are expected to be the electroactive species. Therefore, the values obtained in the present work seem to confirm that the reduction of hemin in aqueous media is followed by the dissociation of dimers, the monomeric hemin being encapsulated in SDS micelles.

## B. Spectral results

The interaction of hemin with SDS was also examined using absorption spectroscopy. Figure 6

shows the results of titration of  $4.4 \times 10^{-5}$  M hemin (in 0.1 M  $\text{KNO}_3$  solution) with  $0 - 2.05 \times 10^{-2}$  M SDS. The spectrum of hemin in aqueous (buffer) solution, was previously analysed by deconvolution<sup>17</sup> and presents the bands of the hemin monomer at 385 nm and that of the  $\mu$ -oxo dimeric species with  $\lambda_{\text{max}} = 342$  nm. Also, the dimerization constant was determined to be

$3.92 \times 10^6 \text{ M}^{-1}$ . In presence of increased concentration of SDS, a sharp hypochromic effect of the hemin monomer and dimer bands is observed, in the premicellar concentration of SDS (Figure 6a). For higher SDS concentrations, the absorption bands increase mostly for the monomer band, which also shifts from 385 nm to 396 nm (Figure 6b).

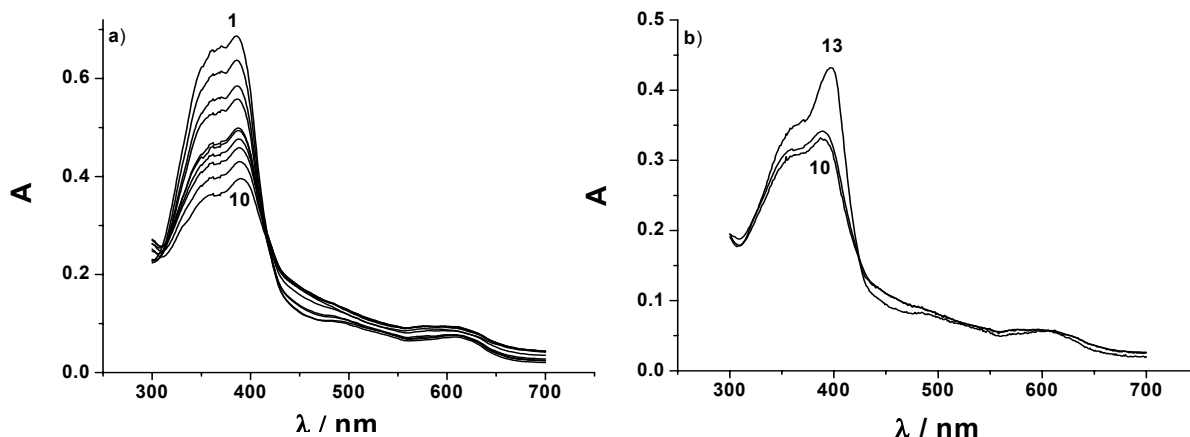


Fig. 6 – Changes in the absorption spectra of hemin in aqueous 0.1  $\text{KNO}_3$  solutions upon titration with SDS at values of concentration in the range of  $0 - 2 \times 10^{-2}$  M; a) Spectra 1 – 10 for  $c_{\text{SDS}} < 8.45 \times 10^{-4}$  M (premicellar range); b) Spectra 10 – 13 for  $c_{\text{SDS}} > 8.45 \times 10^{-4}$  M (micellar range).

The evolution of the absorption spectra of hemin, in function of SDS concentration is presented in Fig. 7 and is quite similar to the variation of the surface tension curve with varying amounts of SDS, in presence of myoglobin.<sup>18</sup>

Three characteristic regions can be delimited with increasing surfactant concentration. At low surfactant concentrations (region I), up to  $3.14 \times 10^{-4}$  M, the absorbance decreases strongly and a small red shift of the Soret band is observed. The hemin, predominantly dimer (90%) in the neutral pH range, may interact with the SDS molecule, which can be interpreted as arising from strong hydrophobic interactions between the detergent and the porphyrin.<sup>4</sup>

Smaller changes in the absorption spectra are observed in the surfactant concentration range from  $3.14 \times 10^{-4}$  M ( $C^1$ ) to  $8.45 \times 10^{-4}$  M ( $C^2$ ) - region II.  $C^1$  – critical aggregation concentration, *cac*, corresponds to the SDS concentration where the hemin-associated micellar aggregates become detectable.<sup>18</sup> The formation of surfactant aggregates does not further perturb the hemin environment. This range correspond to a domain where the surface tension of SDS is practically constant, as shown by literature data in presence of myoglobin.<sup>18</sup>

An important parameter that quantifies hemin-surfactant interaction is the binding ratio<sup>18</sup> defined as:

$$R = \frac{C^2 - C^1}{C_H} \quad (8)$$

where:  $C_H$  is the hemin concentration. In our case the  $R \sim 16$ , that is about 16 SDS molecules are bound per hemin molecule. This ratio corresponds to an average SDS/HEM concentration ratio in region II (from 9 to 27).

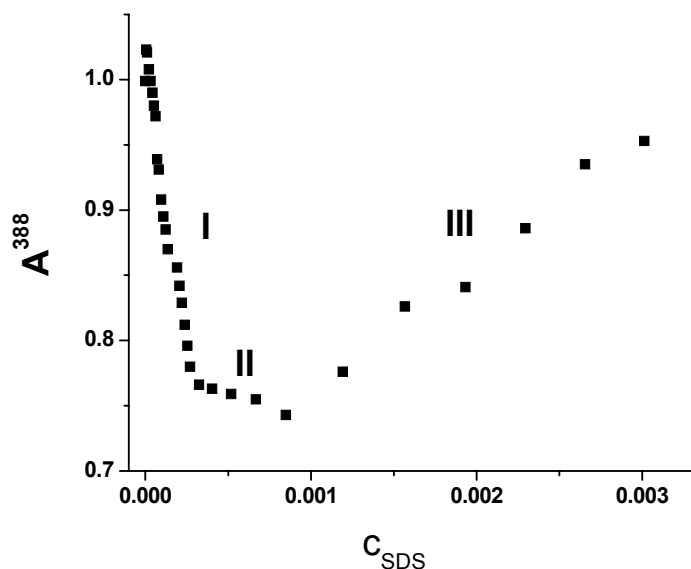
When the SDS concentration reaches the *cmc*\*, the micelles of surfactant are formed, and with higher SDS concentrations (region III) hemin is encapsulated into the micelles, preferentially as monomer.

Considering a 1:1 stoichiometry of the binding process, the association constant  $K$  is given by:

$$K = \frac{c_B}{(c_H^0 - c_B) \times (c_{\text{SDS}}^T - c_B)} \quad (9)$$

\* The *cmc* was calculated with the formula  $\lg \text{cmc} = -3.65 - 0.57 \lg [\text{electrolyte}]$ <sup>19</sup> for different electrolyte concentrations. In our experiments the *cmc* value is in the range of is about  $8.32 \times 10^{-4}$  M –  $1 \times 10^{-3}$  M.

Fig. 7 – Dependence of the absorption  $A$  of hemin in aqueous 0.1  $\text{KNO}_3$  solution on the SDS concentration. The three distinct processes I – III are apparent.



Where  $c_B$  is the concentration of the bound hemin and  $c_{\text{SDS}}^T$  is total concentration of the surfactant. With the assumption that  $c_B \ll c_{\text{SDS}}^T$ , this gives the expression of  $c_B$ :

$$c_B = \frac{K \times c_{\text{SDS}}^T \times c_H^0}{1 + K \times c_{\text{SDS}}^T} \quad (10)$$

The absorbance of the solution at a wavelength in the band of hemin, where the surfactant is supposed not to absorb, is given by:

$$A = \varepsilon_F c_F + \varepsilon_B \quad (11)$$

Taking into account that  $c_H^0 = c_B + c_F$ , the following equation is obtained for the dependence of the absorbance in function of the total SDS concentration:

$$A = \frac{A_0 + \varepsilon_B c_H^0 K_a \times c_{\text{SDS}}^T}{1 + K_a \times c_{\text{SDS}}^T} \quad (12)$$

According to equation (12), a nonlinear regression analysis of the experimental data for regions I and III is presented in Figure 8a, b. For region I (Fig. 8a), an equilibrium constant of  $(1.96 \pm 0.35) \times 10^3 \text{ M}^{-1}$  and  $\varepsilon_B = 9630 \text{ M}^{-1}\text{cm}^{-1}$  are determined. For region III, a 1:1 stoichiometry interaction is considered between the monomeric hemin and the SDS micelle and the following results are obtained:  $K = (0.47 \pm 0.15) \times 10^3 \text{ M}^{-1}$  and  $\varepsilon_B = 41716 \pm 2585 \text{ M}^{-1}\text{cm}^{-1}$ . It should also be noted that the molar absorption coefficient of the bound species is close to the molar absorption coefficient of the free monomer<sup>20</sup>, attesting that the drug is incorporated as monomer in the micelle.

## EXPERIMENTAL

Hemin chloride and SDS were purchased from Sigma and were used without further purification. The stock solution of hemin was prepared by directly dissolving in water (Milli-Q water) containing a small quantity of 0.2 M NaOH and 0.1 M  $\text{KNO}_3$  as supporting electrolyte. The stock solution of SDS was prepared by directly dissolving in pure water.

Cyclic voltammetry experiments with both stationary and rotating disc electrode (RDE) were carried out on a VOLTALAB-32 electrochemical device. The working electrode was a glassy-carbon disc electrode of 3 mm diameter; the reference electrode was a saturated calomel electrode (SCE) and the counter-electrode was a platinum wire electrode. All potential values are reported vs. SCE.

Absorption spectra were recorded with an UNICAM – UV HELIOS spectrophotometer system. Spectral titration is carried out at 20–25°C by starting with a hemin solution and a progressive addition of small aliquots of SDS solution.

The cyclic voltammetry simulations were carried out using DigiSim 3.03 software.<sup>21</sup>

## CONCLUSIONS

The hemin - SDS interaction was studied by cyclic and linear voltammetry with stationary and rotating disc electrode, as well as by absorption spectroscopy. The spectral results outline three processes, in function of the surfactant concentration. Processes I and III were assigned to the interaction between hemin and the molecular SDS, and respectively, between hemin and the SDS micelle and were characterized quantitatively by a 1:1 stoichiometry and the binding constant. The transition region between these processes corresponds to the aggregation domain of the surfactant in presence of hemin, preponderantly

dimeric in solution. In electrochemical experiments, due to the higher concentration of hemin and electrolyte favoring the autoaggregation of heme, only process III is observed and characterised by the binding constant and the diffusion coefficient of the free and bound hemin.

In conclusion, it may be stated that the use of cyclic voltammetry in conjunction with spectral absorption methods, allows a deeper insight in the mechanism of the hemin- surfactant interaction.

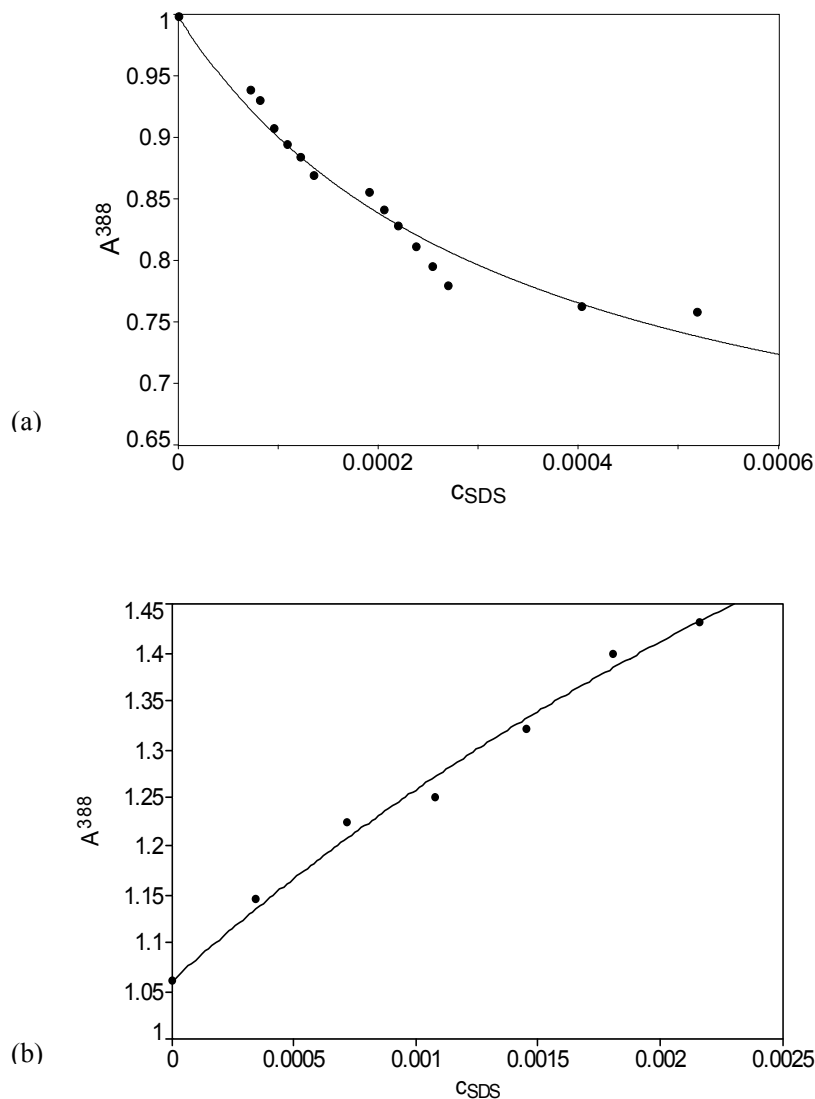


Fig. 8 – Binding curve of hemin to SDS in aqueous 0.1 KNO<sub>3</sub> solution; points represent experimental spectral data and the solid curve represents the fit with eq. [12]: (a) process I; (b) process III.

## REFERENCES

1. C. C. Diaconu, M. Tone, S. M. Ruta, C. Bleotu, C. Cernescu and E. Volanschi, *Proc. Rom. Acad. Series B*, **2005**, *7*, 15-21.
2. C. J. Reedy, M. L. Kennedy and B. R. Gibney, *Chem. Commun.*, **2003**, 570.
3. P. Travascio, Y. Li and D. Sen, *Chemistry and Biology*, **1998**, 505.
4. J. Simplicio, *Biochemistry*, **1972**, *11*, 2525.
5. D. K. Das, C. Bhattaray and O. K. Medhi, *J. Chem. Soc., Dalton Trans.*, **1997**, 4713-4717.
6. J. F. Rusling and M. Y. Brooks, *J. Electroanal. Chem. Interfacial Electrochem.*, **1984**, *163*, 277.
7. K. M. Kadish and J. Jordan, *J. Electrochem. Soc.*, **1978**, *125*, 1250-1257.
8. Q. Feng, N-Q. Li and Y-Y. Jiang, *Analytica Chimica Acta* **1997**, *344*, 97-104.
9. C. F. Kolpin and H. S. Swofford, Jr., *Analytical Chemistry*, **1978**, *50*, 916-920.

10. H. Sun, H. Ma and N. Hu, *Bioelectrochemistry and Bioenergetics*, **1999**, *49*, 1-10.
11. D. K. Gosser Jr., "Cyclic voltammetry: Simulation and analysis of reaction mechanisms", VCH, N. Y., 1993, p. 98-100.
12. A. Bard and R. J. Faulkner, "Electrochemical methods: fundamentals and applications", J. Wiley & Sons, Inc, N. Y., 2001, p. 236, 591-600.
13. A. Bard, "Electroanalytical chemistry", Marcel Dekker, INC, N. Y., 1984, Vol. 13.
14. H. Huck, *Phys. Chem. Chem. Phys.*, **1999**, *1*, 855-859.
15. E. Laviron, *J. Electroanal. Chem.*, **1979**, *101*, 19.
16. D. M. Reza, M-M. A. Akbar, N. Parviz and S. Shahrokh, *J. of Biochem. And Molecular Biology*, **2002**, *35*, 364-370.
17. E. Sahini, M. Dumitrescu, E. Volanschi, L. Barla and C. Diaconu, *Biophysical Chem.*, **1996**, *58*, 245-253.
18. L. Tofani, A. Feis, R. E. Snoke, D. Berti, P. Baglioni and G. Smulevich, *Biophysical Journal*, **2004**, *87*, 1186-1195.
19. M.J. Schick, *J. Phys. Chem.*, **1964**, *68*, 3586.
20. N. Shaklai, Y. Shviro, E. Rabizadeh and I. Kirschner-Zilber, *Biochim. Biophys. Acta*, **1985**, *821*, 355.
21. M. Rudolph, D.P. Reddy and S.W. Feldberg, *Anal. Chem.* **1994**, *66*, 589A.